

NUMERICAL SIMULATIONS OF FEW-MIN OSCILLATIONS IN A GRAVITATIONALLY STRATIFIED SOLAR CORONA

P. KONKOL, K. MURAWSKI

Group of Astrophysics, Institute of Physics
Maria Curie-Skłodowska University in Lublin (UMCS)
Radziszewskiego 10, 20-031 Lublin, Poland

(Received March 7, 2011; revised version received August 24, 2011)

We consider few-min oscillations in a gravitationally-stratified solar corona. These oscillations are triggered by initial pulse in the vertical velocity component that is launched below the transition region. We develop the model in the frame of two-dimensional Euler equations which are solved numerically. Our numerical results reveal that few-min (1–7 min) oscillations are effectively excited by the velocity pulses, with their waveperiod depending on a shape and a vertical position of the initial pulse.

DOI:10.5506/APhysPolB.42.2153

PACS numbers: 95.30.Qd, 96.60.Hv, 96.60.P–

1. Introduction

Waves and oscillations are seen in the solar corona. In particular, 3- and 5-min oscillations are detected in coronal loops (*e.g.* De Moortel *et al.* [1, 2]). Multi wavelength observations of 5-min oscillations in loops were made by Marsh *et al.* [3], and 3- and 5-min oscillations associated with moving magnetic features are observed by Lin *et al.* [4]. The propagating upward slow magnetoacoustic waves with periods of about 5 min were detected in the transition region and coronal emission lines by Hinode/EIS at the footpoint of a coronal loop that was rooted at plage (Wang *et al.* [5]).

It is apparent that 5-min period corresponds to the main period of p-modes, which may serve as a potential explanation of the coronal oscillations. However, in a case of gravitationally stratified atmosphere the dispersion relation for vertical acoustic waves can be derived from the Klein–Gordon equation, which results in cut-off wave period P_{ac} smaller than 5 min (*e.g.* Lamb [6] and Roberts [7]). As waves are able to propagate for their wave periods smaller than P_{ac} we infer that the 5-min oscillations are not

able to penetrate into the solar corona. Bel and Leroy [8] suggested that the cut-off frequency of magnetic field-free atmosphere is lower when waves propagate with the angle to the vertical. McIntosh [9] found the observational justification of the modification of the cut-off frequency along inclined magnetic field. De Pontieu *et al.* [10] proposed that as a result of fall-off of acoustic cut-off frequency, p-modes may be channeled into the solar corona along inclined magnetic field lines. The oscillations then may be steepened into shocks, producing spicules (Murawski, Zaqarashvili [11]). De Pontieu *et al.* [10] argued that the observed quasi 5-min period in spicule appearance is associated with the periodicity of p-modes. Zaqarashvili *et al.* [12] proposed that 5-min oscillations in the solar corona are originated from granules which were modeled by a vertical propagating wavefront in the vertical velocity component. However, Zaqarashvili *et al.* [12] considered a simple one dimensional (1D) problem of 5-min oscillations. The 1D case treats the acoustic waves only while the internal gravity waves are inherently removed from the system. Therefore there is a need to consider a 2D scenario in which both acoustic and internal gravity waves are present.

The aim of this paper is to extend the 1D model of Zaqarashvili *et al.* [12] on the 2D hydrodynamical case and show that 1–7-min oscillations can be effectively triggered by two-dimensional (2D) pulses in the vertical component of velocity. This paper is organized as follows. The numerical model is described in Sect. 2. The numerical results are presented and discussed in Sect. 3. This paper is completed by conclusions in Sect. 4.

2. A numerical model

2.1. Euler equations

Our model system is taken to be composed of a gravitationally-stratified solar atmosphere that is described by the 2D Euler equations:

$$\frac{\partial \varrho}{\partial t} + \nabla \cdot (\varrho \mathbf{V}) = 0, \quad (1)$$

$$\varrho \frac{\partial \mathbf{V}}{\partial t} + \varrho (\mathbf{V} \cdot \nabla) \mathbf{V} = -\nabla p + \varrho \mathbf{g}, \quad (2)$$

$$\frac{\partial p}{\partial t} + \nabla \cdot (p \mathbf{V}) = (1 - \gamma)p \nabla \cdot \mathbf{V}, \quad (3)$$

$$p = \frac{k_B}{m} \varrho T. \quad (4)$$

Here ϱ is the mass density, $\mathbf{V} = [V_x, V_y, 0]$ is the flow velocity, p is the gas pressure, T is the temperature, $\gamma = 5/3$ is the adiabatic index, $\mathbf{g} = (0, -g, 0)$ is gravitational acceleration with its value $g = 2.74 \times 10^2 \text{ m s}^{-2}$, m is the mean particle mass and k_B is Boltzmann's constant.

2.2. Initial configuration

2.2.1. The equilibrium

We assume that at the equilibrium the solar atmosphere is a still ($\mathbf{V} = \mathbf{0}$) environment with gas pressure and mass density given as

$$p(y) = p_0 \exp\left(-\int_{y_r}^y \frac{dy'}{\Lambda(y')}\right), \quad \varrho(y) = \frac{p(y)}{g\Lambda(y)}. \quad (5)$$

Here

$$\Lambda(y) = \frac{k_B T(y)}{mg} \quad (6)$$

is the pressure scale-height, and p_0 denotes the gas pressure at the reference level, $y = y_r = 10$ Mm.

We adopt a realistic temperature profile $T(y)$ for the solar atmosphere (Vernazza *et al.* [13]). This profile is displayed in Fig. 1. Note that T attains a value of about 5700 K at the top of the photosphere which corresponds to $y = 0.5$ Mm. At higher altitudes $T(y)$ falls off until it reaches its minimum of 4350 K at the altitude $y \simeq 0.95$ Mm. Higher up $T(y)$ grows gradually with height up to the transition region which is located at $y \simeq 2.7$ Mm. Here $T(y)$ experiences a sudden growth up to the coronal value of 1.5 MK at $y = 10$ Mm.

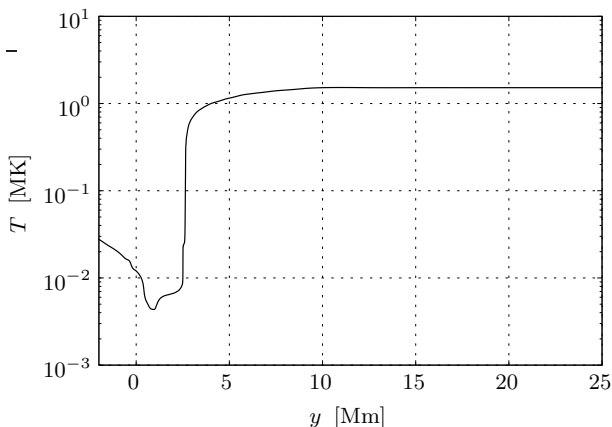


Fig. 1. Equilibrium temperature T (in mega Kelvins) *versus* height y (in Mm) for the solar atmosphere.

Having specified $T(y)$ with a use of Eq. (5) we can obtain mass density and gas pressure profiles as seen in Fig. 2. Both $p(y)$ and $\varrho(y)$ experience a sudden fall-off from photosphere to coronal values at the transition region.

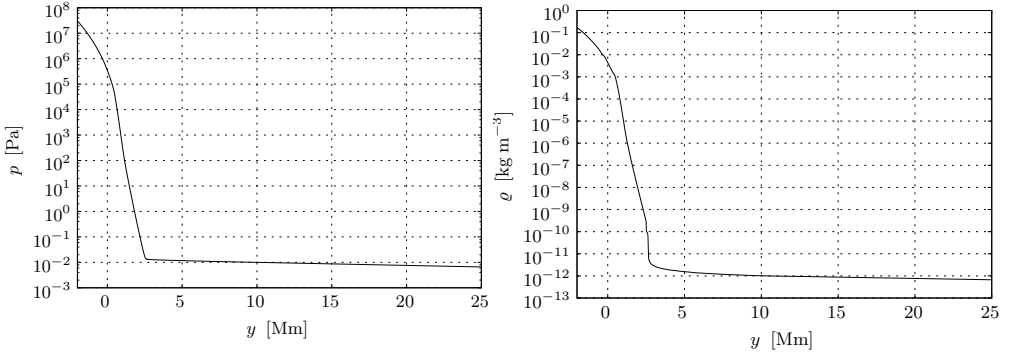


Fig. 2. Equilibrium profiles of gas pressure p (left) and mass density ρ (right).

This type of fall-off results in the cut-off frequency

$$\Omega_{\text{cut-off}}(y) = \frac{c_s(y)}{2\Lambda(y)} \sqrt{1 + 2\Lambda'(y)}. \quad (7)$$

Here the squared sound speed, c_s^2 , is given as

$$c_s^2(y) = \frac{\gamma p(y)}{\rho(y)}. \quad (8)$$

Figure 3 displays the acoustic cut-off period $P_{\text{cut-off}} = 2\pi/\Omega_{\text{cut-off}}$ of the model atmosphere *versus* height. In the low chromosphere $P_{\text{cut-off}} \simeq 200$ s and then it quickly increases towards the corona. Note that $P_{\text{cut-off}}$ attains a value of about 200 s at $y = 0.5$ Mm. It grows to the transition region where it reaches coronal values such as at $y = 10$ Mm $P_{\text{cut-off}} = 3.5 \times 10^3$ s. It is noteworthy that Eq. (7) is obtained from the linear analysis, while the nonlinear description changes the oscillation period of a wave (Zaqarashvili *et al.* [12]).

2.2.2. Perturbations

We excite waves in the above described solar atmosphere by launching initially, at $t = 0$ s, the impulse in a vertical component of velocity V_y , *i.e.*

$$V_y(x, y, t = 0) = A_v \exp \left[-\frac{x^2}{w_x^2} - \frac{(y - y_0)^2}{w_y^2} \right]. \quad (9)$$

Here A_v is the amplitude of the initial Gaussian pulse, y_0 its initial vertical position and w_x and w_y its widths in the x - and y -directions. The case of $w_x \rightarrow \infty$ corresponds to a horizontal wave-front, which was discussed by Zaqarashvili *et al.* [12]. As a consequence of that we can compare our results with the numerical findings of Zaqarashvili *et al.* [12].

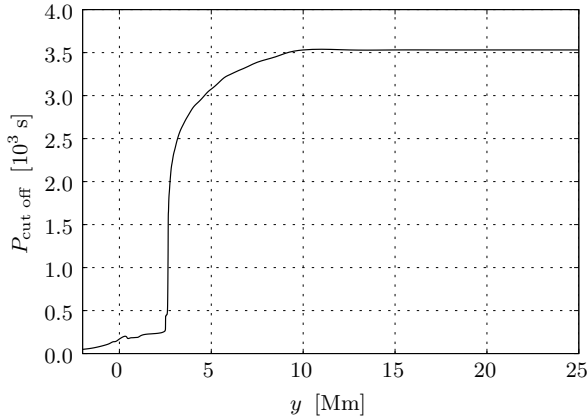


Fig. 3. Acoustic cutoff wave period $P_{\text{cut-off}}$ (in units of 10^3 s) versus height y (in Mm).

3. Numerical results

We solve equations (1)–(4) numerically, using the code FLASH (Dubey *et al.* [14]) which implements a second-order unsplit Godunov solver and Adaptive Mesh Refinement (AMR). We set the simulation box as $(-6, 6)$ Mm \times $(-0.5, 12.5)$ Mm. At all boundaries we fix all plasma quantities to their equilibrium values. In our studies we use AMR grid with a minimum (maximum) level of refinement blocks set to 3 (10). The refinement strategy is based on controlling numerical errors in a gradient of temperature. Such settings result in an excellent resolution of steep spatial profiles, which significantly reduces numerical diffusion within the simulation region.

Figure 4 illustrates spatial profiles of the total velocity $|V|$ and velocity vectors at $t = 180$ s, $t = 250$ s, $t = 350$ s and $t = 700$ s for the initial pulse amplitude $A_v = 2$ km s $^{-1}$, pulse width $w_x = w_y = 0.1$ Mm and its vertical position $y_0 = 0.5$ Mm. Left panels show, the whole simulation region and the right ones the zoomed region around localized perturbation. The initial pulse splits in a usual way into counter-propagating waves. The waves propagating upwards grow in their amplitudes as a result of the rapid decrease of mass density in the chromosphere (Zaqarashvili *et al.* [12]). As a consequence there appears a shock. Photospheric and chromospheric plasma is lifted up by gas pressure which settles in below the shock. The pressure gradient force overwhelms gravity and it pushes the photospheric and chromospheric material towards the solar corona (Murawski and Zaqarashvili [11]). At a later time the plasma becomes attracted by gravity and as a result it falls off towards the low layers. It is noteworthy here that Kelvin–Helmholtz (KH) instabilities seed in, similarly as it was observed by Gruszecki *et al.* [15].

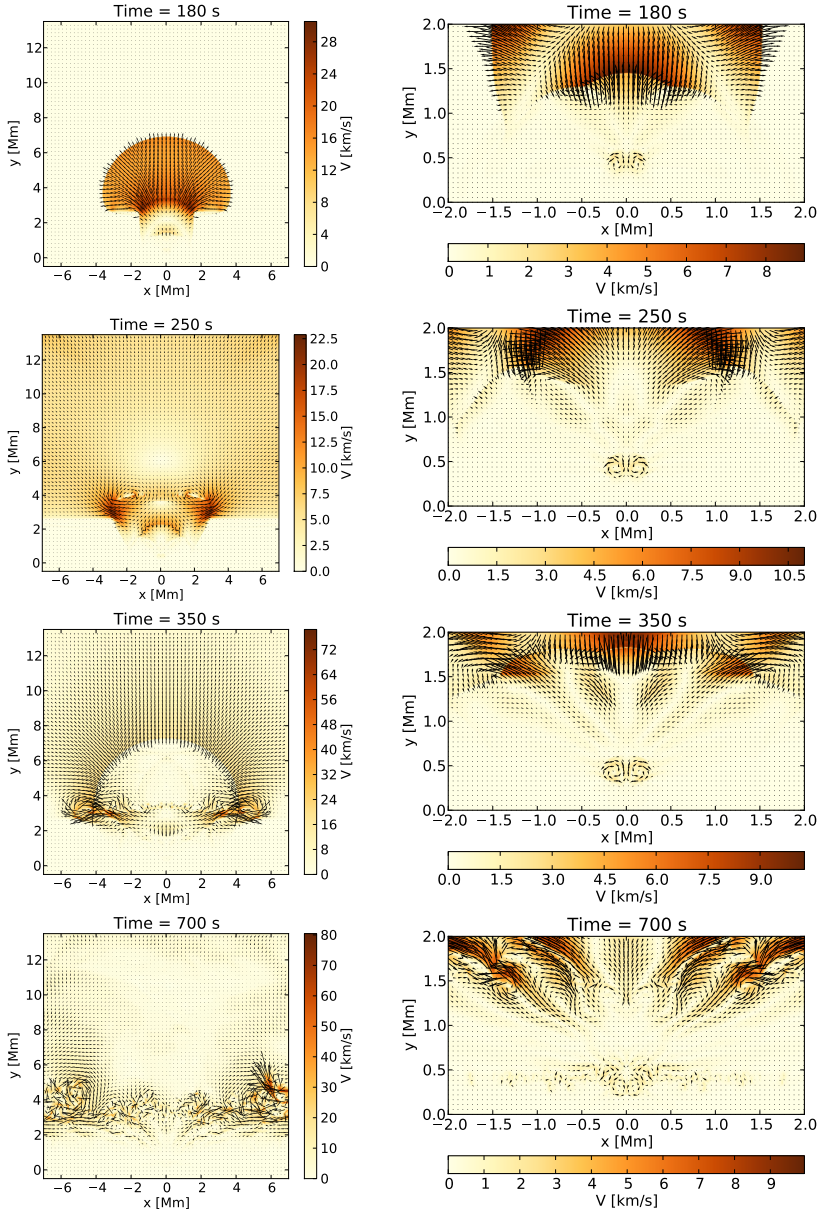


Fig. 4. Total velocity $|V(x, y)|$ (colour maps) and velocity vectors (arrows) at (from top to bottom) $t = 180$ s, $t = 250$ s, $t = 350$ s and $t = 700$ s, for $y_0 = 0.5$ Mm, $w_x = w_y = 0.1$ Mm and $A_v = 2 \text{ km s}^{-1}$. Right panels display the zoomed region. Velocity is expressed in units of 1 Mm s^{-1} . Velocity vectors are drawn in units of 50 km s^{-1} (left panels) and 10 km s^{-1} (right panels).

As a result of these instabilities vortices emerge which at $t = 350$ s are clearly visible at $(x = \pm 4, y = 3)$ Mm and $(x = 0, y = 0.5)$ Mm. The secondary shock which results from the original pulse works against the fall-off of plasma as it lifts up the photospheric and chromospheric region. This is clearly seen at about $t = 350$ s when a complex bi-directional flow arises. The whole scenario bears some features of small jets which were recently studied by Murawski and Zaqarashvili [11] and we refer the interested reader to this paper for more detailed description of the plasma evolution in the context of a simpler equilibrium temperature albeit magnetically permeated plasma model.

Figure 5 displays time-signatures of the vertical component of velocity, V_y , for the case of Fig. 4. This velocity is collected along the line $x = 0$ Mm (top panel) and at the detection point $(x = 0, y = 12)$ Mm (bottom panel). The arrival of the leading shock front to the detection point occurs at $t \simeq 217$ s. The second, third, and fourth shocks fronts reach the detection point at $t \simeq 389$ s, $t \simeq 473$ s, and $t \simeq 634$ s, respectively. This secondary shock results from the nonlinear wake which lags behind.

Figure 6 displays time span Δt between first two shock arrival times to the detection point *versus* vertical position of the initial pulse y_0 . For the case of localized pulse (dots) which is launched from $y_0 = 0$ Mm, $\Delta t = 200$ s. This value is close to $P_{\text{cut-off}}(y = 0)$ of Fig. 3. For larger values of y_0 , Δt grows slightly until it reaches its maximum of $\Delta t = 210$ s at $y_0 \simeq 0.2$ Mm. At higher altitudes Δt declines slowly to about 60 s for $y_0 = 2$ Mm. Note that in the case of the wave-front (crosses), that corresponds to the 1D case discussed by Zaqarashvili *et al.* [12], $\Delta t \simeq 440$ s for $y_0 = 0$ Mm. At $y_0 = 0.2$ Mm Δt attains its minimum of $\Delta t = 400$ s. Higher up it grows with y_0 until at $y_0 = 0.5$ Mm Δt attains its maximum of $\Delta t \simeq 470$ s, and subsequently it subsides with height y_0 , falling off to $\Delta t \simeq 140$ s for $y_0 = 1.5$ Mm.

4. Conclusions

There are few conclusions which can be drawn from our simulations:

- (a) A small amplitude initial pulse launched below the transition region exhibits a tendency to generate shocks *e.g.*, Zaqarashvili *et al.* [12]. These shocks result from finite-amplitude waves which originate from the initial pulse. Amplitude of these waves grow with height as the result of the mass density fall-off;
- (b) When initially pushed up, cold plasma begins to fall-off gravitationally and Kelvin–Helmholtz instabilities may seed in, that results in a development of vortices, similarly as reported by Gruszecki *et al.* [15];

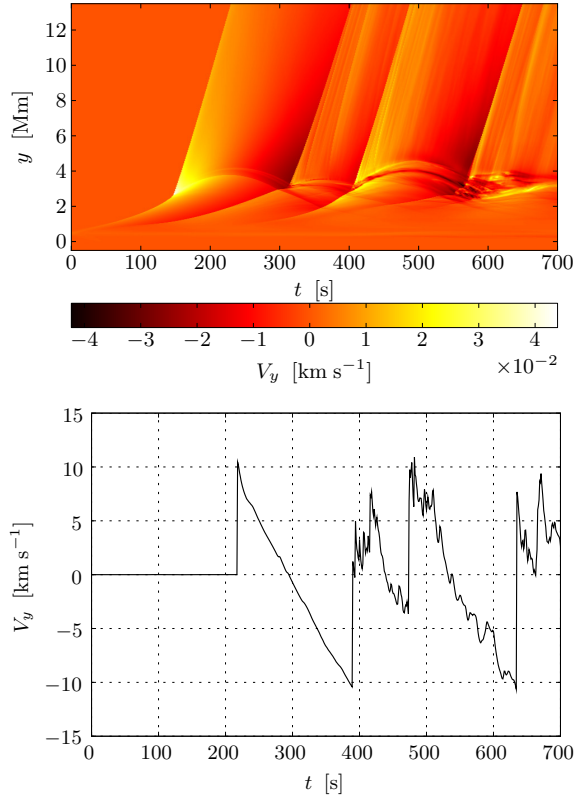


Fig. 5. Time-signatures of V_y (in units of km s^{-1}) collected along $x = 0$ Mm (top panel) and at $(x = 0, y = 12)$ Mm (bottom panel) for the case of Fig. (4).

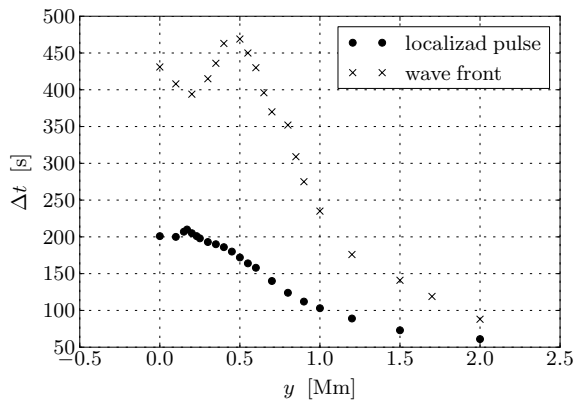


Fig. 6. Arrival time between first two shocks *versus* impulse initial position y_0 .

- (c) The waveperiod of oscillations, which are detected in the solar corona, depends on a shape and vertical location of the initial pulse. A localized pulse results in wave-periods within the range of 1–4 min, while a horizontal wave-front is able to excite larger wave-period (2–7 min) oscillations. It is noteworthy here that as the case of a horizontal wave-front corresponds to the 1D case we were able to confirm the results of Zaqarashvili *et al.* [12]. Shorter wave period oscillations are triggered by impulses which are initially launched higher up in the solar atmosphere.

The authors express their cordial thanks to Dr. Teimuraz Zaqarashvili and Prof. Leon Ofman for stimulating discussions.

REFERENCES

- [1] I. De Moortel, J. Ireland, R.W. Walsh, *Astron. Astrophys.* **355**, L23 (2000).
 [2] I. De Moortel, J. Ireland, A.W. Hood, R.W. Walsh, *Astron. Astrophys.* **387**, L13 (2002).
 [3] M.S. Marsh, R.W. Walsh, I. De Moortel, J. Ireland, *Astron. Astrophys.* **404**, L37 (2003).
 [4] C.H. Lin, D. Banerjee, E. O’Shea, J.G. Doyle, *Astron. Astrophys.* **460**, 597 (2006).
 [5] T.J. Wang, L. Ofman, J.M. Davila, *Astrophys. J.* **696**, 1448 (2009).
 [6] H. Lamb, *Proc. London Math. Soc.* **7**, 122 (1908).
 [7] B. Roberts, in Proc. SOHO 13 Waves, Oscillations and Small-Scale Transient Events in the Solar Atmosphere: A Joint View from SOHO and TRACE, Palma de Mallorca, Spain, (ESA SP-547), 1, 2004.
 [8] N. Bel, B. Leroy, *Astron. Astrophys.* **55**, 239 (1977).
 [9] S.W. McIntosh, S.W. Jefferies, *Astrophys. J.* **647**, L77 (2006).
 [10] B. De Pontieu, R. Erdélyi, S.P. James, *Nature* **430**, 536 (2004).
 [11] K. Murawski, T. Zaqarashvili, *Astron. Astrophys.* **519**, A8 (2010).
 [12] T.V. Zaqarashvili, K. Murawski, M.K. Khodachenko, D. Lee, *Astron. Astrophys.* **529**, A85 (2011).
 [13] J.E. Vernazza, E.H. Avrett, R. Loeser, *Astrophys. J.* **45**, 635 (1981).
 [14] A. Dubey *et al.*, *Parallel Computing* **35**, 512 (2009).
 [15] M. Gruszecki, K. Murawski, A. Kosovichev, K. Parchevsky, *Acta Phys. Pol. B* **42**, 1333 (2011).